

DESY Summerstudent Programme
2008
Work Report

Scalar Field Inflation Models

Stephanie Häffner (Friedrich-Alexander-Universität Erlangen-Nürnberg)
Supervisor: Laura Covi (Theorie Gruppe, DESY Hamburg)

September 14, 2008

Contents

1	Introduction	3
2	Inflation Models with Scalar Fields	3
2.1	Slow Roll Approximation	3
2.2	Inflationary models	4
2.2.1	Large Field Models	4
2.2.2	Small Field Models	4
2.2.3	Hybrid models	4
2.2.4	Classification by End of Inflation	5
2.3	Spectrum and spectral index	5
3	Oscillations in the CMB Spectrum	5
3.1	The tanh-Potential	6
3.2	The sin-Potential	6
3.3	The spiky primordial spectrum	7
3.4	CMB Spectra of the Different Primordial Spectra	8
3.4.1	CMB spectra with WMAP5 data	8
3.5	Conclusion	11

1 Introduction

In the first part of this work report I like to introduce some aspects of inflationary models with scalar fields and the slow roll approximation that sometimes can be used to get easy a primordial fluctuation spectra from a potential. With the measurement of the cosmic microwave background (CMB) with COBE later with WMAP one got possibilities to test different models with the data. In the second part of this report I compare the primordial spectra of three different models that lead to oscillations in the CMB spectrum and also the resulting CMB spectra of these models with WMAP5 data.

2 Inflation Models with Scalar Fields

In the Big Bang model there is an epoch of fast expansion that is called inflation. The idea of inflation is favored by many authors because it can solves many problems like the flatness problem, horizon problem and others (see e.g [1], [2],[3] and other cosmological textbooks). Scalar models are one possibility to describe an inflationary phase. The inflation in the simplest model is caused by a scalar field which is rolling down from an local minimum to an global one. This can be described by an “slow-roll approximation” (see chapter 2.1). There are different kinds of scalar field models, which are shortly described in section 2.2. Some of the models describe inflation with more than one scalar field.

2.1 Slow Roll Approximation

Inflation is defined as an era of repulsive gravity with $\ddot{a} > 0$, where $a(t)$ is the scale factor. If the total density Ω_{tot} is close to 1, so we have an flat universe, the evolution of an scalar field ϕ and the scale factor a is given [1]

$$\ddot{\phi} + 3H\dot{\phi} + V' = 0 \quad (1)$$

$$3H^2 = 3\left(\frac{\dot{a}}{a}\right)^2 = \frac{1}{2}\dot{\phi}^2 + V(\phi) \quad (2)$$

where an overdots denotes derivative with respect to the time and an prime with respect to the field ϕ and H is the Hubble parameter. The equation of motion for a spatial homogeneous scalar field can be derived from the action $S = \int d^4x \sqrt{g} [\frac{1}{2} \partial_\mu \phi \partial^\mu \phi + V(\phi)]$ and the field equations [2]. $\sqrt{g} = a^3$ and comes from the Friedman-Robertson-Walker metric.

The scalar field is slowly rolling down its potential and herefore the condition is $\dot{\phi}^2 \ll V(\phi)$ and also the potential of the scalarfield should be flat and $\ddot{\phi}$ should also be $\ll V(\phi)$ [2]. The slow roll parameters are defined [3], [1]

$$\epsilon(\phi) = \frac{M_p^2}{2} \left(\frac{V'}{V}\right)^2 \quad (3)$$

$$\eta(\phi) = M_p^2 \frac{V'''}{V} \quad (4)$$

For the slow roll approximation it is necessary to hold these conditions:

$$\epsilon(\phi) \ll 1 \text{ and } |\eta(\phi)| \ll 1.$$

One can show, if the slow roll approximation is valid, then inflation is guaranteed [3].

2.2 Inflationary models

There were many different scalar field models for an inflationary scenario discussed in literature and there are many possibilities to classify these models. In this chapter I will use the characterization by potential form and initial conditions [2] (see also [6]) and the characterization by end of inflation [4].

2.2.1 Large Field Models

Potentials of this kind are usually used in “chaotic” inflation scenarios (for further information about chaotic inflation see [5]). In the chaotic inflation scenario the Universe evolved from a quantum gravitational state with energy density comparable to Planck scale. Here are mainly exponentially potentials $V(\phi) = \lambda^4 \exp(\phi/\mu)$ and polynomial potentials $V(\phi) = \lambda^4 (\phi/\mu)^p$ used. For large field models is $V''(\phi) > 0$ and $-\epsilon < \delta = \eta - \epsilon < \epsilon$. The simplest chaotic inflation model has the potential $V(\phi) = m^2 \phi^2/2$.

2.2.2 Small Field Models

In this class of models are potentials used that arise from spontaneous symmetry breaking e.g. original models of “new” inflation and “natural” inflation. Here have the potentials the form $V(\phi) = \lambda^4 [1 - (\mu/\phi)^p]$. This potential form can also be viewed as a lowest order Taylor expansion of an arbitrary potential about the origin. For this kind of potentials is $V''(\phi) < 0$, $\eta < -\epsilon$ and ϵ close to zero. The inflaton field in small field models starts from near an unstable equilibrium and rolls down the potential to a stable minimum.

2.2.3 Hybrid models

Most models that are used in hybrid inflation are of the form $V(\phi) = \lambda^4 [1 + (\phi/\mu)^p]$, but there are also used other potentials e.g $V(\phi) \propto \ln(\phi)$ in models with Supersymmetry or $V(\phi) \propto \phi^{-p}$ in intermediate inflation and dynamical supersymmetric inflation. Here is $V''(\phi) > 0$ and $0 < \epsilon < \delta$. In typical hybrid inflation models are more than one scalar field involved.

2.2.4 Classification by End of Inflation

Another way to classify the different inflation models is the ending of the inflation phase. There are two possibilities: ending of slow roll phase versus phase transitions. Models, in that the inflation ends with slow rollover, describe an slow rolling inflaton field which rolls to the minimum and oscillates there. Models, that end with phase-transition, need at least two fields. One field is the slow rolling inflaton field while the other field triggers the end of inflation, here are also oscillations in the end. There exist models with Einstein gravity and with extended gravity theories like Supergravitation.

2.3 Spectrum and spectral index

The spectrum of primordial curvature perturbation in the slow-roll approximation is given by [3]

$$P_R(k) = \frac{1}{12\pi^2 M_{Pl}^6} \frac{V^3}{V'^2} = \frac{1}{24\pi^2 M_{Pl}^4} \frac{V}{\epsilon} \quad (5)$$

evaluated at the epoch of horizon exit $k = aH$. The value of ϕ at this epoch can be obtained by [9]

$$\ln\left(\frac{k_{end}}{k}\right) = N(k) = M_P^{-2} \int_{\phi_{end}}^{\phi} \frac{V}{V'} d\phi \quad (6)$$

The scale dependence of the spectrum is described by the scale-dependent spectral index n [3]:

$$n_s - 1 = 2\eta - 6\epsilon \quad (7)$$

With gauge-invariant computation of the curvature perturbation one can find [2]

$$P_R(k) = A_s^2 \left(\frac{k}{a \cdot H}\right)^{n_s - 1} \quad (8)$$

The newest data show (WMAP5 [14]) a spectral index $n_s = 0.96$.

There are also tensor perturbations generated by the quantum oscillations, but the spectrum of tensor perturbations is much smaller than the scalar spectrum. The ratio of theses spectrum is $P_{grav(k)}/P_R(k) = \epsilon$ and is negligible for $\epsilon \ll 1$. The scalar to tensor ratio at low l is also defined as [9]

$$r = \frac{C_l^{grav}}{C_l^R} = 12.4\epsilon \quad (9)$$

3 Oscillations in the CMB Spectrum

In this chapter I discuss three different primordial spectra with the CMB spectrum, that was measured by WMAP. Each of these primordial spectra leads to oscillations in the CMB spectrum and in the COBE and WMAP data there are some evidences for oscillations at lower l . The physical motivation for looking into the oscillations at low l is that many of the primordial spectra that causes oscillations in the CMB spectra arise from models with more than one field.

3.1 The tanh-Potential

The first model is a chaotic inflationary potential $m^2\phi^2$ with an added step at $\phi = b$ [10]. Inflationary models with a step can naturally arise in theories with many interacting fields, e.g. in supergravity models [11]. Each step corresponds to a symmetry-breaking phase transition in a field coupled to the inflaton [10].

$$V(\phi) = \frac{1}{2}m^2\phi^2\left(1 + \tanh\left(\frac{\phi - b}{d}\right)\right) \quad (10)$$

b and d are in units of the Planck mass M_p . This potential can not be treated in the slow-roll approximation and the primordial potential $P(k)$ was derived and discussed e.g. in [11]. In the same publication is also a discussion of the best fit values for the parameters b , c and d . I approximated the spectrum $P(k)$ for the values $m = 7.5 \cdot 10^{-6}$, $b = 14$, $c = 10^{-3}$ and $d = 2 \cdot 10^{-2}$ with

$$P_R(k) = 1.65 \cdot 10^{-9} \begin{cases} k^{n_s-1} & \text{if } k < 0.0008 \\ k^{n_s-1} + e^{-250k} \sin(1.2 - 1500 \cdot k) & \text{if } k \leq 0.0008 \end{cases} \quad (11)$$

with $n_s = 0.96$.

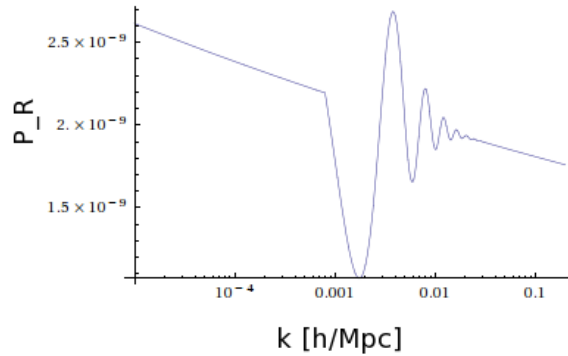


Figure 1: primordial spectrum constructed for the tanh potential

3.2 The sin-Potential

The second model is similar in the form to the tanh-model, because it also contains the standard chaotic potential $m^2\phi^2$, but now with additional oscillations:

$$V(\phi) = \frac{1}{2}m^2\phi^2\left(1 + a \cdot \sin\left(\frac{\phi}{b} + \delta\right)\right) \quad (12)$$

This model is discussed in [12] with $\delta = 0$, $a = 5 \cdot 10^{-4}$, $b = 3 \cdot 10^{-2}$ and $m = \sqrt{8 \cdot \pi} \cdot 10^{-6}$. In this publication the spectrum of the model was received with numerical methods. For this work I got spectrum mostly analytically from this potential but with one approximation.

This potential can be treated in the slow roll approximation (see chapter 2.3). The spectrum of the primordial curvature perturbations is given in equation 5. To evaluate the right-hand side of this equation, one has to solve

$$55 - \ln\left(\frac{k}{a_0 H_0}\right) = N(k) = M_P^{-2} \int_{\phi_{end}}^{\phi} \frac{V}{V'} d\phi \quad (13)$$

where a_0 is the scale factor today, i.e. $a_0 = 1$ and $H_0 = (h/3000) \text{ Mpc}^{-1}$ with $h = 0.72$. For this potential is an analytical solution of the integral not possible. Numerically treatment shows an linear connection between integral value and ϕ for the relevant scale for inflation with $k = 40 \dots 50$. With the linear approximation one can estimate $\phi(k)$ and gets for the spectrum

$$P_R(k) \approx \frac{1.7 \cdot 10^{-35} \cdot \phi(k)^6 \left(1 + \frac{\sin(1.4 \cdot 10^{-17} \phi)}{2000}\right)^3}{(5.1 \cdot 10^5 \cdot \phi(k)^2 \cdot \cos(1.4 \cdot 10^{-17} \phi(k)) + 1.5 \cdot 10^{26} \phi(k) \left(1 + \frac{\sin(1.4 \cdot 10^{-17} \phi)}{2000}\right))^2} \quad (14)$$

with

$$\phi(k) \approx 3.35 \cdot 10^{17} (1.1 \cdot 10^2 - \log\left(\frac{k}{a_0 H_0}\right)) \quad (15)$$

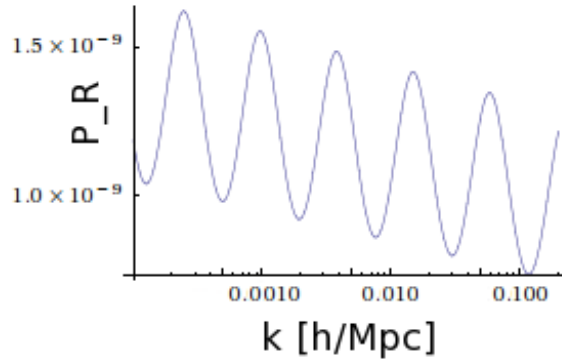


Figure 2: primordial spectrum of the sin potential

An comparison of this primordial spectrum with the primordial spectrum in [12] shows, that here the frequency of the oscillations is little higher and the amplitude is less than there. These could be effects of the linear approximation, that was made in the calculations of the spectrum.

3.3 The spiky primordial spectrum

Another primordial spectrum that also leads to oscillations in the CMB spectrum was discussed in [13], that contains an spike and an dip. They assume an initial power

spectrum with spiky corrections:

$$P(k) = A_s \cdot k^{n-1} \left(1 + \sum_i \alpha_i \exp\left(-\frac{(k - k_{ci})^2}{2\sigma_i^2}\right) \right) \quad (16)$$

where A_s is the amplitude of primordial fluctuations and n is the spectral index. Both values one can get from COBE or WMAP data. I choose the same parameters like in [13] to get an dip and an spike: $\alpha_1 = 3.0$, $k_{c1} = 4.3 \cdot 10^{-3} h \text{ Mpc}^{-1}$, $\sigma_1 = 7.5 \cdot 10^{-5} h \text{ Mpc}^{-1}$ and $\alpha_2 = -0.9$, $k_{c2} = 2.5 \cdot 10^{-3} h \text{ Mpc}^{-1}$, $\sigma_2 = 1.4 \cdot 10^{-4} h \text{ Mpc}^{-1}$.

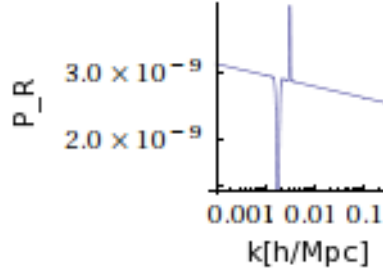


Figure 3: primordial spectrum with dip and spike

3.4 CMB Spectra of the Different Primordial Spectra

The primordial spectra, that are discussed above are very different, but each of them leads to some oscillations in the resulting CMB spectra. The CMB spectra were created with CMBFAST version 4.5.1.

3.4.1 CMB spectra with WMAP5 data

In figure 4 are showed the resulting CMB spectra for the different primordial spectra that were introduced above. For a better comparison there is also the CMB spectrum of the primordial powerlaw spectrum $\propto k^{n_s-1}$. I used the WMAP 5 data [14] with $h = 0.705$, $\Omega_\Lambda = 0.726$, $\Omega_b = 0.046$, $\Omega_{CDM} = 0.228$, $\tau = 0.084$ and $z_{reion} = 10.9$. For reionization I used the RECFAST routine in CMBFAST.

In table 1 are the positions of the first three peaks of the CMB spectra for the different models and in table 2 are the amplitude ratios for these peaks. There are strong deviation for the sin model at the peak positions and amplitude ratios to the power law model, that describes the peak positions and amplitude ratios of the data very good.

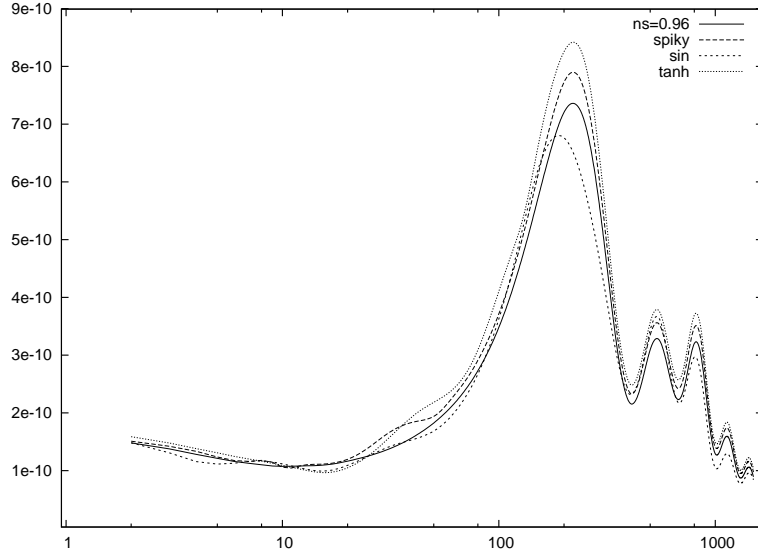


Figure 4: CMB spectra of the different primordialspectra

Peak Position	Peak 1	Peak 2	Peak 3
$n_s = 0.96$	220	538	815
spiky	220	538	813
sin	189	536	807
tanh	221	537	814

Table 1: peak positions of in the different CMB spectra

Amplitude Ratio	Peak 1	Peak 2	Peak 3
$n_s = 0.96$	1	0.44665	0.439028
spiky	1	0.450836	0.444468
sin	1	0.546465	0.436223
tanh	1	0.450217	0.442508

Table 2: peak amplitude ratios in the different CMB spectra

In figure 5 are plotted the different CMB Spectra with the WMAP5 binned data, but without the sin CMB spectrum, because it does not describe the peak positions and amplitude of the data very well. One can see in this figure that at high $l > 60$ there are

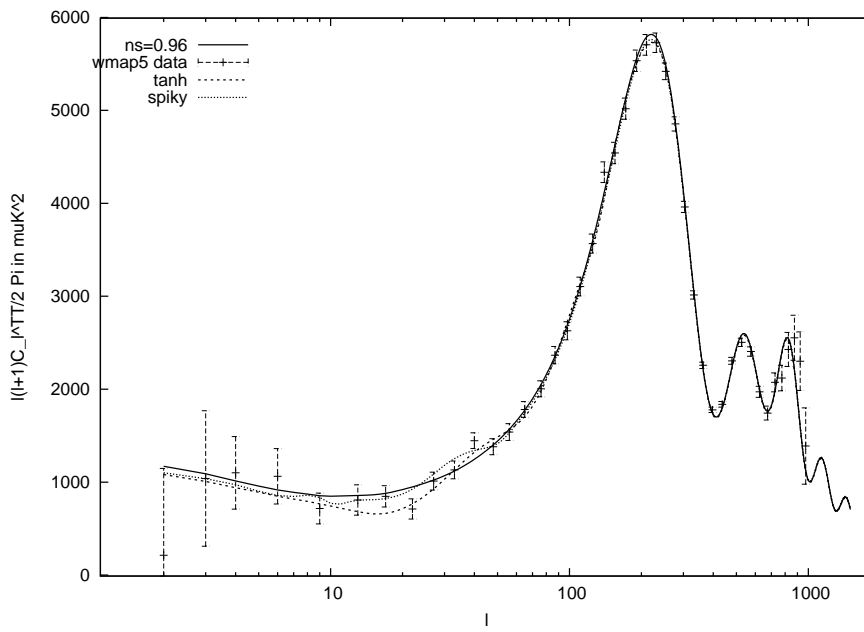


Figure 5: CMB spectra with the WMAP 5 binned data

almost no differences in the resulting CMB spectra of the different primordial spectra. At small l are differences between the different models, but none of the different CMB spectra matches all data points within the errorbars.

3.5 Conclusion

For the comparison of the different CMB spectra I used for each model the parameters from the cited publications. The choosen parameters in these publications were from fits of the model to the data with Markov Chain Monte Carlo (MCMC) simulations. But not all of the parameters I used were fitted to WMAP5 data but also to WMAP3 data (tanh model) or WMAP1 data (spiky model) and I used these parameters to get the CMB spectrum with some cosmological parameters from the WMAP5 data. I also used for the tanh model not the numerically achieved primordial spectrum, but made an approximation with an piecewise function and with the sin model I made an linear approximation during the calculation of the primordial spectrum and got so not exactly the same primordial spectrum like [12]. I would have to make my own MCMC simulations to get the best fit parameters to the WMAP5 data and only after this I can get a significant comparison between the CMB spectra of these models.

References

- [1] D.H.Lyth and A. Riotto, *Phys. Rept.* **314** (1999)
- [2] A. Riotto, hep-ph/0210162
- [3] A.R. Liddle and D.H. Lyth, “*Cosmological Inflation and Large-Scale Structure*”, Cambridge University Press, (2000)
- [4] A. Linde, *Phys. Rev. D* **49**,748 (1994)
- [5] A.D. Linde, *Phys. Lett. B* **129**, 177 (1983)
- [6] S. Dodelson, W.H. Kinney, E.W. Kolb, *Phys. Rev. D* **56**, 3207 (1997)
- [7] E.J.Copeland, A.R.Liddle, D.H.Lyth, E.D.Stewart and D.Wands, *Phys. Rev. D* **49**, 6410 (1994)
- [8] T. Asaka, W.Buchmüller and L. Covi, *Phys. Lett. B* **510**, 271 (2001)
- [9] L.Covi, hep-ph/0111365
- [10] J.A.Adams, B.Cresswell and R. Easther, *Phys. Rev. D* **64** 1235141 (2001)
- [11] L.Covi, J.Hamann, A. Melchiorri, A. Slosar and I. Sorbera, *Phys.Rev. D* **74** 083590 (2006)
- [12] C.Pahud, M. Kamionkowski and A. R. Liddle, astro-ph 0807.0322
- [13] M. Kawasaki, F. Takahashi and T. Takahashi, *Phys. Lett. B* **605** 223 (2005)
- [14] C.L Bennet et al., astro-ph 0803.0586